Proceedings of the International School of Physics "Enrico Fermi"
Course 190 "Frontiers in Modern Optics", edited by D. Faccio, J. Dudley and M. Clerici
(IOS, Amsterdam; SIF, Bologna) 2016
DOI 10.3254/978-1-61499-647-7-159

Quantum interference and imaging

M. Lahiri(*)

Vienna Center for Quantum Science and Technology (VCQ), Faculty of Physics
University of Vienna - Boltzmanngasse 5, Vienna A-1090, Austria

C. Reimer

INRS-EMT, 1650 Boulevard Lionel-Boulet
Varennes, Québec J3X 1S2, Canada

A. Zeilinger(**)

Vienna Center for Quantum Science and Technology (VCQ), Faculty of Physics
University of Vienna - Boltzmanngasse 5, Vienna A-1090, Austria

Institute for Quantum Optics and Quantum Information
Austrian Academy of Sciences - Boltzmanngasse 3, Vienna A-1090, Austria

Quantum Optics, Quantum Nanophysics, Quantum Information
University of Vienna - Boltzmanngasse 5, Vienna A-1090, Austria

Summary. — We give an overview of the quantum theory of interference and show that this has important practical implications. We discuss an imaging technique that was designed and based on the principles of quantum mechanics.

(*) E-mail: mayukh.lahiri@univie.ac.at
(**) E-mail: anton.zeilinger@univie.ac.at

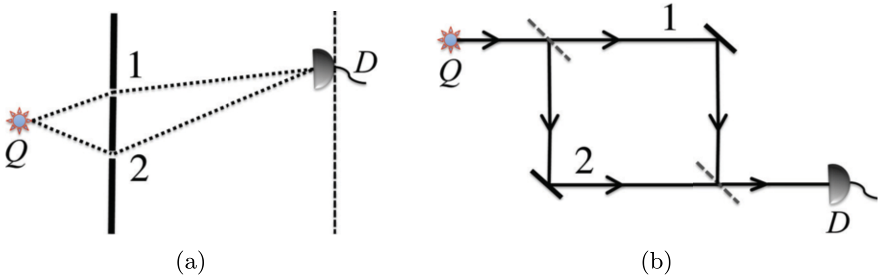

Fig. 1. – (a) Young's double slit experiment. (b) Mach-Zehnder interference experiment.

1. – Introduction

In order to understand the behavior of a quantum system or entity, one needs "a combined use of the contrasting pictures" of a classical particle and a classical wave [1]. Wave-particle duality is one of the central concepts of quantum mechanics. In spite of being taught in every elementary courses on quantum mechanics, wave-particle duality remains counter-intuitive and, as newer experiments are being performed, continues to call for a deeper level of understanding.

It is well known that quantum-mechanical descriptions of interference experiments are based on the wave-particle duality of quantum entities (see, for example, [2, 3]). In this paper, we give a simple overview of the quantum-mechanical interpretation of interference and its application to an imaging experiment. Our aim is not to provide a rigorous theoretical treatment that would require the use of quantum field theory. We rather aim to show how important physical results can be understood by basic principles and simple arguments.

In sect. **2** we discuss the related basic concepts and results of an experiment. In sect. **3** we then show how these concepts can be used to design an imaging experiment. We also discuss the novelty of the imaging experiment in sect. **4**.

2. – Interference and path information

2˙1. *Basic concept.* – Let us consider a situation in which a quantum entity is emitted by a source, Q, and then detected by a detector D. Suppose that the entity can take two alternative paths, 1 and 2, to arrive at D; for example, as in a Young's double-slit experiment (fig. 1(a)) or in a Mach-Zehnder interferometer (fig. 1(b)). If the probability of detecting the entity at D when it travels via path 1 is $P_1 = |\alpha_1|^2$, we say that the corresponding *probability amplitude* is α_1. Here α_1 is, in general, a complex number. P_1 is directly proportional to the counting rate of D when path 2 is blocked. Similarly, the probability of detecting the quantum entity at D when it travels via path 2 is given by $P_2 = |\alpha_2|^2$, with the corresponding probability amplitude α_2. When interference occurs, the total probability of the entity being detected at D is given by

$$P = |\alpha_1 + \alpha_2|^2 = P_1 + P_2 + 2\sqrt{P_1 P_2}\cos\phi, \tag{1}$$

where $\phi = \arg\{\alpha_1^* \alpha_2\}$, "arg" being the argument of a complex number. According to quantum mechanics, interference occurs if and only if there is absolutely no possibility of determining which path the quantum entity takes to arrive at D. In other words, interference occurs if and only if there is no *path information* anywhere in the universe. When the path information is available, no interference occurs, *i.e.*, the probability of detecting the quantum entity at D is given by

$$P = |\alpha_1|^2 + |\alpha_2|^2 = P_1 + P_2. \tag{2}$$

It is important to understand that this information does not need to be extracted by a measurement; the presence of the path information alone is enough to destroy the interference. In Feynman's words [2]: "Nature does not know what you are looking at, and she behaves the way she is going to behave whether you bother to take down the data or not."

An interesting situation arises if we allow the possibility of the path information being "partially available". In order to understand this case, we need a measurable quantity to quantify the quality of interference. Such a quantity, called *visibility*, is given by

$$\mathcal{V} \equiv \frac{P_{\max} - P_{\min}}{P_{\max} + P_{\min}}. \tag{3}$$

Here $P_{\max}$ and $P_{\min}$ are the maximum and minimum values of P, respectively. It is evident that $0 \le \mathcal{V} \le 1$.

If $P_1 = P_2$, it follows from eqs. (1) and (3) that $\mathcal{V} = 1$, *i.e.*, complete unavailability of the path information under ideal conditions leads to perfect interference characterized by unit visibility. Similarly, using eqs. (2) and (3), it can be verified that complete availability of the path information implies zero visibility.

It is also possible to have a case where the visibility is less than unity but more than zero. In such a case, if $P_1 = P_2 = P_0$, say, the total probability of detecting a quantum entity a D is given by

$$P = 2P_0(1 + \mathcal{V}\cos\phi). \tag{4}$$

We can generalize eq. (4) to include the possibility of $P_1 \neq P_2$. The equation can now be expressed in the form

$$P = P_1 + P_2 + 2\mathcal{V}_0\sqrt{P_1 P_2}\cos\phi, \tag{5}$$

where

$$\mathcal{V}_0 = \left(\frac{P_1 + P_2}{2\sqrt{P_1 P_2}}\right)\mathcal{V}. \tag{6}$$

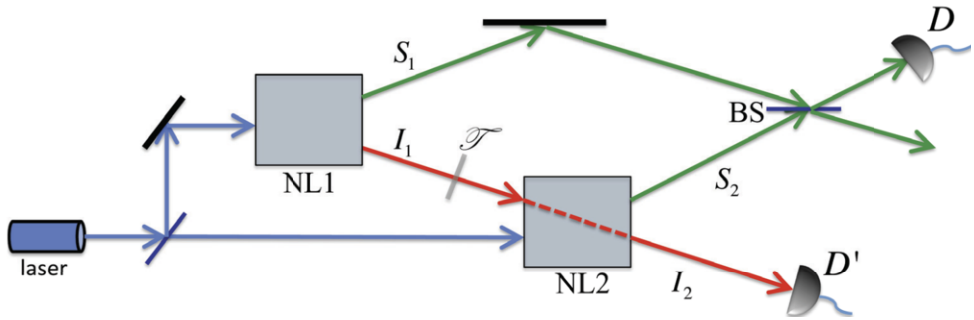

Fig. 2. – An illustration of the experiment performed in ref. [8]. No coincidence detection is performed. The presence of D' is not actually required; it is shown only to illustrate the role of path information in the experiment.

In such situations, we say that the path information is partially available. Quantum-mechanical interpretation of interference thus allows us to consider $\mathcal{V}_0$ as a measure of unavailable path information (for further discussions, see [4-7]).

2˙2. *Application to an optical interference experiment.* – The quantum-mechanical interpretation of interference can be applied to explain any lowest-order interference experiment performed in optics. However, in most cases the same experiments can also be explained by classical electromagnetic theory without any reference to the postulates of quantum mechanics. We now discuss an interference experiment which can only be explained by the use of quantum theory. The experiment was originally performed by Zou, Wang, and Mandel [8, 9] and is one of the most mind-boggling experiments in the history of quantum optics.

The experimental setup is illustrated in fig. 2. Two *identical* nonlinear crystals NL1 and NL2 are illuminated by laser light beams generated by the *same* source. We call the laser beam “pump”. A pump photon is converted into a photon pair by the process of spontaneous parametric down-conversion inside these crystals(1). We call the two down-converted photons “signal” and “idler”. The sum of the energies of signal and idler photons is equal to the energy of a pump photon. This is because the process of parametric down-conversion conserves energy. The signal and idler produced by NL1 are denoted by S_1 and I_1, respectively. Similarly, S_2 and I_2 represent the signal and idler generated by NL2.

We superpose the S_1 and S_2 beams by a beam splitter, BS, and collect the superposed light emerging from one of the outputs of BS by a detector, D. We measure the photon counting rate at D. If the rate of down-conversion at both crystals is very low, it is highly improbable for a photon pair emitted by NL1 and a photon pair emitted by NL2 to be simultaneously present in the system. This experiment can, therefore, be considered as

(1) There are numerous scientific documents written on the theory of parametric down-conversion (see, for example, [10-14]; see also [15, 16]).

a single-photon interference experiment. If it is possible (even in principle) to determine from which crystal the photon was originated, the path information for a signal photon arriving at D becomes fully available. In this case, no interference will occur. Since the signal photons emitted by the two crystals are identical in all aspects (for example, same polarization, frequency, etc.), it is not possible to determine the path information by measurements performed only on signal photons. However, since each signal and idler pair is produced simultaneously in a particular crystal, the path information can be extracted by detecting both photons by the method of coincidence detection(2). Therefore, if we want to observe interference at D, we need to design the experiment in such a way that the path information cannot be obtained by coincidence detection.

Let us send I_1 photon beam through NL2 and align it with I_2 photon beam. Suppose that t_0, t_1, and t_2 are the propagation times of I_1 from NL1 to NL2, of S_1 from NL1 to D, and of S_2 from NL2 to D, respectively. If the path lengths for S_1, S_2, and I_1 are chosen such that $t_1 - t_2 - t_0 = 0$, there is no way to distinguish a signal photon generated by NL1 from a signal photon generated by NL2(3). This fact can be easily justified by a simple argument. Suppose that a detector, D', collects both I_1 and I_2 photons emerging from NL2 (fig. 2). If the time taken by I_1 to travel from NL1 to D' is t'_1 and the travel time of I_2 from NL2 to D' is t'_2, we have $t'_1 - t'_2 = t_0$. When signal and idler photons belonging to a photon pair generated by NL1 are detected at D and D', respectively, the time difference between the two detections is $t_1 - t'_1$. Similarly, for a photon pair generated by NL2, the time difference between their detections at D and D' is $t_2 - t'_2$. Therefore, when $t_1 - t'_1 = t_2 - t'_2$, *i.e.*, when $t_1 - t_2 - t_0 = 0$, it is not possible to say whether a coincident count is due to a photon pair from NL1 or a photon pair from NL2. In this case, perfect interference is observed at D, because no path information is available. It must be noted that the presence of detector D' or the measurement of coincidence counts is absolutely not required. In fact, no coincidence measurement is performed to observe the interference.

If the I_1 beam is completely blocked between NL1 and NL2, it becomes possible to extract the path information by coincidence measurement; in this case, no interference is observed at D. Again, the presence of D' is not at all required to observe this effect, because availability of path information is enough to destroy interference even if we choose not to extract the information by measurement.

Suppose now that we place an attenuator, $\mathscr{T}$, on the path of I_1 between NL1 and NL2 (fig. 2). The amplitude transmission coefficient of the attenuator is T, which implies that the intensity of I_1 beam drops by a factor of $|T|^2$ when it passes through $\mathscr{T}$. Since a photon cannot be broken into further fractions, an idler photon can either be fully transmitted or fully blocked by $\mathscr{T}$. We cannot control the transmission or blocking of photons individually. We can only say that the probability of an idler photon being

(2) For a discussion of coincidence detection see [15], sect. 14.7.1.
(3) In practice it is enough for $|t_1 - t_2 - t_0|$ to be much less than the coherence time of the down-converted light [9].

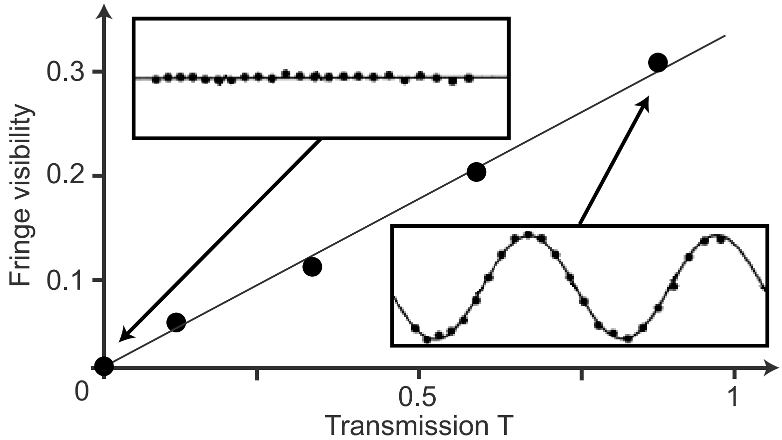

Fig. 3. – Experimentally measured visibility as a function of $|T|$. This confirms that the visibility is proportional to $|T|$. (Figure generated by combing figs. 2 and 3 of [8].)

transmitted through $\mathscr{T}$ is $|T|^2$. Because of this, we have neither full path information nor no path information; we have something in between: partial path information. As expected, we obtain less than unity value for the visibility in this case. It can be shown by explicit calculation that the photon counting rate (*i.e.*, the probability of detecting a photon) at D has the form [8, 9]

$$P = P_1 + P_2 + 2|T|\sqrt{P_1 P_2}\cos\left(\arg\{T\} + \phi_0\right), \tag{7}$$

where P_1 is the photon counting rate when S_2 beam is blocked, P_2 is the photon counting rate when S_1 beam is blocked, and ϕ_0 is an interferometric phase term. (Note the similarity between eqs. (5) and (7).) It is important to note that the values of P_1 and P_2 do not depend on whether I_1 beam is blocked or not. It is clear from eq. (7) that the visibility is directly proportional to $|T|$. This is exactly what was observed in the experiment (fig. 3).

It follows from the discussion above that $|T|$ provides a measure of the unavailable path information. In other words, availability of the path information can be controlled by using attenuators of different transmittance values. The fact that the visibility is directly proportional to $|T|$ is the key feature of this experiment. It can be shown that this fact cannot be explained by classical electromagnetic theory [17].

3. – A quantum imaging experiment

It follows from eq. (7) that the visibility of the interference fringes at D depends on the modulus and the phase of the attenuator's amplitude transmission coefficient (see fig. 2). This fact can be used to develop an imaging technique which is essentially different from all standard ones [18].

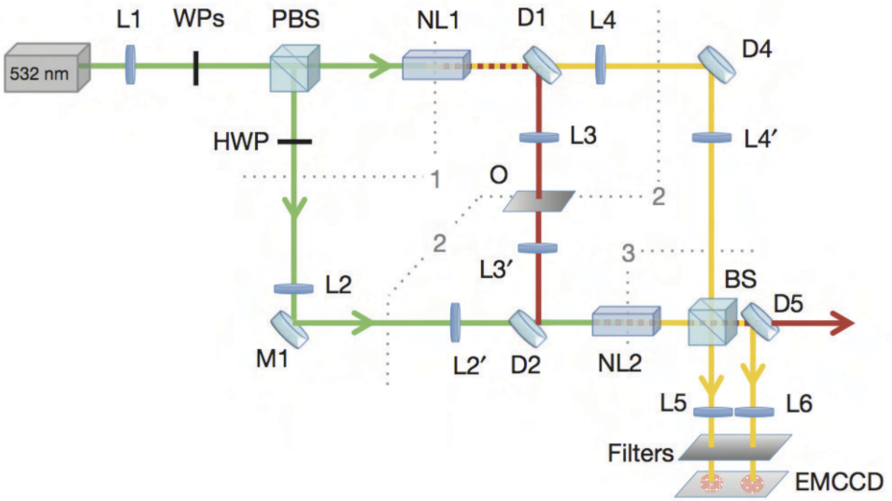

Fig. 4. – A continuous-wave 532 nm laser (green) illuminates crystals NL1 and NL2. Wave plates (WPs) adjust the relative phase and intensity of the outputs of the polarizing beam splitter (PBS). The dichroic mirror D1 separates down-converted 810 nm (yellow) and 1550 nm (red) photons. The 1550 nm photons (idler) are transmitted through the object O and sent through NL2 by dichroic mirror D2. Lenses image plane 1 onto plane 3, and plane 2 onto the EMCCD camera. The positive lenses L3, L3′, L4, L4′ have the same focal length f_I; positive lenses L5 and L6 have the focal length f_0. A 50:50 beam splitter (BS) combines the 810 nm beams. Dichroic mirrors D1, D2, D4 and D5 transmit the pump. (Adapted from [18].)

The experimental setup used in the imaging experiment (fig. 4) is constructed by making the following modifications to the experimental setup described in fig. 2: 1) NL1 and NL2 generate signal and idler photons of wavelengths $\bar{\lambda}_S = 810\,\text{nm}$ and $\bar{\lambda}_I = 1550\,\text{nm}$, respectively, by *collinear* spontaneous parametric down-conversion; 2) the attenuator is replaced by the object to be imaged; 3) appropriate lens systems are used; 4) the detector D is replaced by a camera situated at the back focal plane of a positive lens; 5) both outputs of the beam splitter, BS, are collected by the camera.

The amplitude transmission coefficient of the object (O) is denoted by $T(\boldsymbol{\rho}_{\text{ob}})$, where $\boldsymbol{\rho}_{\text{ob}}$ is a two-dimensional position vector representing a point of the object. It can be shown by rigorous calculations that the probability of detecting a signal photon at a point on the camera (camera pixel) can be expressed in the form [19]

$$P_+(\boldsymbol{\rho}_{\text{im}}) \approx P_1 + P_2 + 2\sqrt{P_1P_2}|T(\boldsymbol{\rho}_{\text{ob}})|\cos(\arg[T(\boldsymbol{\rho}_{\text{ob}})]), \tag{8a}$$

$$P_-(\boldsymbol{\rho}_{\text{im}}) \approx P_1 + P_2 - 2\sqrt{P_1P_2}|T(\boldsymbol{\rho}_{\text{ob}})|\cos(\arg[T(\boldsymbol{\rho}_{\text{ob}})]), \tag{8b}$$

where $\boldsymbol{\rho}_{\text{im}}$ is the position vector of the camera pixel, and the subscripts $+$ and $-$ represent two outputs of BS. Equations (8) imply that both absorptive ($\arg[\mathscr{T}(\boldsymbol{\rho}_{\text{ob}})] = 0$) and phase ($|\mathscr{T}(\boldsymbol{\rho}_{\text{ob}})| = 1$) objects can be imaged by this system. They further imply that the image

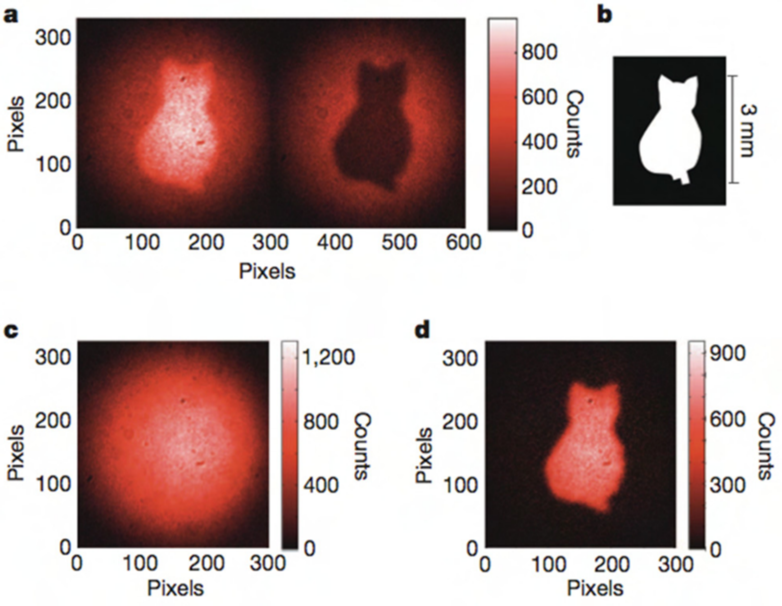

Fig. 5. – a) Images appearing at the two outputs of BS. b) The absorptive object made by removing the silhouette of a cat from a piece of cardboard. c) The sum of the outputs gives the intensity profile of the signal beams without any image. d) The subtraction of the outputs leads to an enhancement of the interference contrast. (Adapted from [18].)

appears in the camera for both outputs of BS. Summing up the two outputs completely removes the image. The fact that the object information appears only in the interference term shows that the imaging process is purely quantum mechanical.

Figure 5 shows the images of an absorptive object. The object is a rectangular piece of cardboard from which the silhouette of a cat has been cut out and removed (fig. 5(b)). Images obtained at the two outputs of BS are shown in fig. 5(a). When the two outputs are summed, the image disappears (fig. 5(c)). When one of the outputs is subtracted from the other, the image contrast is enhanced (fig. 5(d)).

Figure 6 shows images of a phase object. The chosen object (fig. 6(b)) introduces a relative phase shift of approximately 2π for 810 nm light, and is therefore not visible if placed in the signal beam between lenses L4 and L4′. However, the same object produces approximately π phase shift for 1550 nm light, and is therefore clearly visible if placed in the idler beam between lenses L3 and L3′ (fig. 6(a)).

Finally, fig. 7 shows images of a phase object that is opaque to light of 810 nm wavelength. It is, therefore, impossible to realize transmission imaging by illuminating the silicon with 810 nm photons. However, we can obtain the image of this object by placing it on the idler beam (1550 nm).

The different wavelengths of signal ($\bar{\lambda}_S$) and idler ($\bar{\lambda}_I$) photons also play a role in the image magnification. It can be shown by explicit calculation that the magnification is

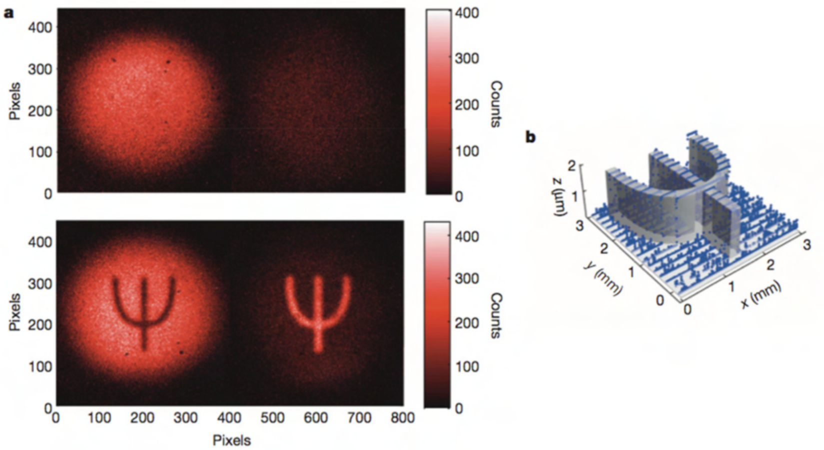

Fig. 6. – a) Top picture: no image is obtained when the object is placed in the signal beam (820 nm) beam between L4 and L4′. Bottom picture: images are obtained at both outputs of BS when the object is placed in the idler beam (1550 nm). b) The phase object. (Adapted from [18].)

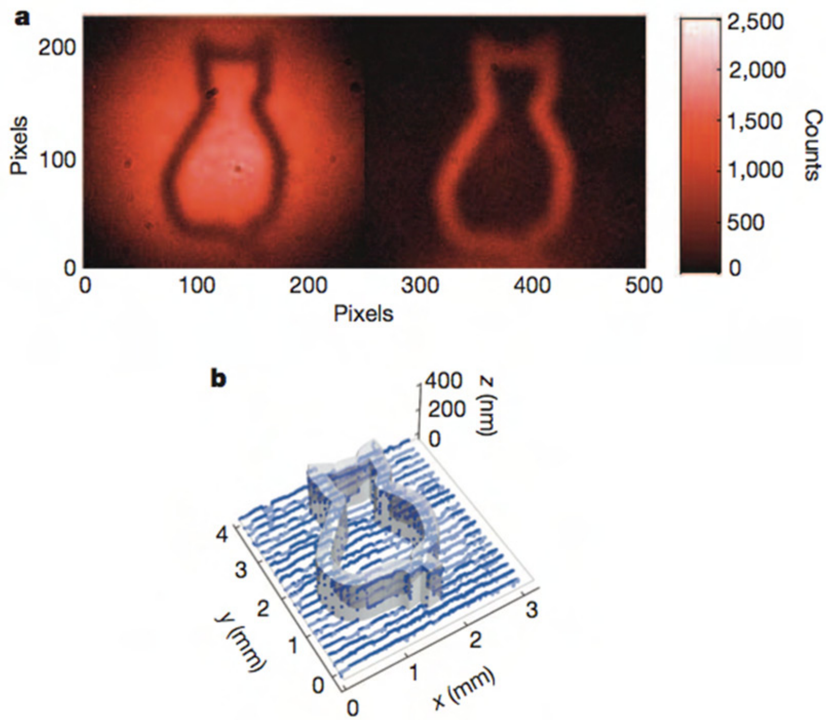

Fig. 7. – a) Images obtained at both outputs of BS. b) The phase object that is opaque to 810 nm light. (Adapted from [18].)

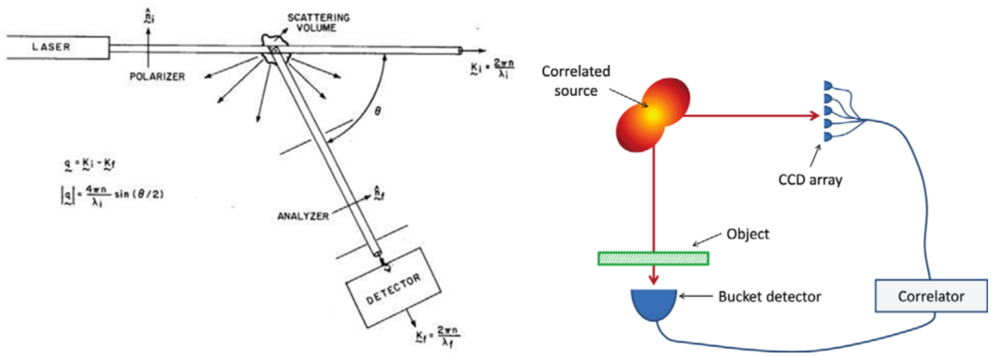

(a) (b)

Fig. 8. – (a) A scattering experiment (adapted from [20]). (b) Illustrating principles of ghost imaging. (Adapted from [24].)

given by [19]

$$M = \frac{f_0 \bar{\lambda}_S}{f_I \bar{\lambda}_I}, \tag{9}$$

where f_0 and f_I are defined in the caption of fig. 4. This value of the magnification has also been confirmed experimentally.

4. – Novelty of the imaging experiment

It is clear from the above discussions that the principle behind our imaging experiment is purely quantum mechanical. It is important to note that the interference of signal beams occurs *not* because of stimulated down-conversion at NL2, but because of the unavailability of path information. In this context, let us have another look at fig. 5, which shows images of an absorptive object. This object is a rectangular piece of cardboard from which a cat silhouette has been removed. Idler photons pass through this hollow shape inside the cardboard, and interference occurs at the corresponding points (pixels) on the camera. Outside the hollow shape, all idler photons are blocked, and no interference occurs at the corresponding points on the camera. The image of the hollow shape appears on the camera due to the occurrence or non-occurrence of interference.

As mentioned earlier, we make no attempt to extract the path information by detecting the idler photons. Since the object is illuminated only by the idler photons, we have thus designed an imaging experiment in which the light interacting with the object is never detected. This fact is a unique feature of our imaging technique. All other existing imaging techniques are based on the detection of the photons that are interacting with the object. The most common imaging technique involves scattering experiments in which the radiation interacting with the object must be detected for constructing an image (fig. 8(a)). A more recent imaging technique, widely known as ghost imaging [21-24], also requires the detection of the photons that interact with the object (fig. 8(b)). In this sense, our imaging technique is fundamentally different from all other existing techniques.

5. – Conclusion

We have given a basic overview of the quantum theory of interference. We have also shown that it is possible to design an imaging experiment which is exclusively based on the principles of quantum mechanics. Our discussion shows that the quantum-mechanical interpretation of interference phenomena is not only an academic topic but can also have practical applications. Although we have refrained from entering into a rigorous theoretical analysis, we encourage the reader to consult the cited scientific articles for further reference.

* * *

The research of M.L. and A.Z. is supported by ÖAW, the European Research Council (ERC Advanced grant no. 227844 "QIT4QAD", and SIQS grant no. 600645 EU-FP7-ICT), and the Austrian Science Fund (FWF) with SFB F40 (FOQUS) and W1210-2 (CoQus). M.L. thanks A. Hochrainer, R. Lapkiewicz, and G. B. Lemos for numerous discussions.

REFERENCES

[1] Bohr N., *Discussion with Einstein on epistemological problems in atomic physics*, in *Albert Einstein: Philosopher-Scientist*, edited by Schilpp P. A., *Library of Living Philosophers*, Vol. **VII** (Open Court Publishing Company) 1949.
[2] Feynman R. P., Leighton R. B. and Sands M., *The Feynman Lectures on Physics*, Vol. **III** (Addison-Wesley Publishing Company, New York, USA) 1966.
[3] Scully M. O., Englert B.-G. and Walther H., *Nature*, **351** (1991) 111.
[4] Greenberger D. M. and Yasin A., *Phys. Lett. A*, **128** (1988) 391.
[5] Mandel L., *Opt. Lett.*, **16** (1991) 1882.
[6] Jaeger G., Shimony A. and Vaidman L., *Phys. Rev. A*, **51** (1995) 54.
[7] Englert B.-G., *Phys. Rev. Lett.*, **77** (1996) 2154.
[8] Zou Z. Y., Wang L. J. and Mandel L., *Phys. Rev. Lett.*, **67** (1991) 318.
[9] Wang L. J., Zou Z. Y. and Mandel L., *Phys. Rev. A*, **44** (1991) 4614.
[10] Louisell W. H., Yariv A. and Siegman A. E., *Phys. Rev.*, **124** (1961) 1646.
[11] Gordon J. P., Louisell W. H. and Walker L. R., *Phys. Rev.*, **129** (1963) 481.
[12] Kleinman D. A., *Phys. Rev.*, **174** (1968) 1027.
[13] Mollow B. R., *Phys. Rev. A*, **8** (1973) 2684.
[14] Hong C. K. and Mandel L., *Phys. Rev. A*, **31** (1985) 2409.
[15] Mandel L. and Wolf E., *Optical Coherence and Quantum Optics* (Cambridge University Press, Cambridge) 1995.
[16] Boyd R. W., *Nonlinear Optics* (Academic Press) 2008, ISBN 978-0123694706.
[17] Wiseman H. M. and Mølmer K., *Phys. Lett. A*, **270** (2000) 245.
[18] Barreo Lamos B., Borish V., Cole G. D., Ramelow S., Lapkiewicz R. and Zeilinger A., *Nature*, **512** (2014) 409.

[19] Lahiri M., Lapkiewicz R., Lemos G. B. and Zeilinger A., *Phys. Rev. A*, **92** (2015) 013832.
[20] Berne B. and Pecora R., *Dynamic Light Scattering: With Applications to Chemistry, Biology, and Physics* (Dover, Mineola, NY) 2000.
[21] Pittman B., Shih Y. H., Strekalov D. V. and Sergienko A. V., *Phys. Rev. A*, **52** (1995) 3429.
[22] Bennink R. S., Bentley S. J. and Boyd R. W., *Phys. Rev. Lett.*, **89** (2002) 113601.
[23] Gatti A., Brambilla E., Bache M. and Lugiato L. A., *Phys. Rev. Lett.*, **93** (2004) 093602.
[24] Rogy S. and Adesso G., *Sci. Rep.*, **1** (2012) 651.